Matematisk-fysiske Meddelelser
udgivet af
Det Kongelige Danske Videnskabernes Selskab
Bind **33,** nr. 12

Mat. Fys. Medd. Dan. Vid. Selsk. **33,** no. 12 (1963)

THE INFRARED SPECTRUM OF CH_3D

BY

FLEMMING ALLAN ANDERSEN

København 1963
i kommission hos Ejnar Munksgaard

CONTENTS

Page

I. Introduction 3

II. Experimental 4
1. Preparations 4
2. Spectroscopic Procedure 5

III. Fundamental Bands 5
1. Parallel Bands (A_1 Fundamentals) 5
2. Perpendicular Bands (E Fundamentals) 8
3. Results 30

IV. Overtones and Combinations 32

References 35

Synopsis

The infrared spectrum of CH_3D has been measured in the region 400–6000 cm^{-1} by means of a prism instrument (Beckman IR 3) of medium resolving power. The band-centre frequencies have been derived by rotational analysis of the fundamental bands. The results are compared with previous prism and grating data, and a slightly revised set of normal vibration frequencies is given.

A value of the rotational constant $A''(A_0)$ has been obtained, which agrees within the limits of error with a recent Raman value.

Coriolis coupling constants have been derived for the three doubly degenerate fundamentals.

Possible assignments of the observed combination bands are given.

Printed in Denmark
Bianco Lunos Bogtrykkeri A-S

I. Introduction

The infrared and Raman spectra of methane and its deuterated species, CH_3D, CH_2D_2, CHD_3, and CD_4, have been the object of several investigations.[1] However, when one examines the literature, it is obvious that several of the fundamental frequencies of the partly deuterated methanes are uncertain. As the investigations cited above[1] of these molecules are now more than 20 years old and the experimental technique since then has improved considerably, a re-investigation of all the fundamental bands of the partly deuterated methanes appeared to be desirable.

In 1953 BOYD and THOMPSON[2] and later ALLEN and PLYLER[3] (1959) have measured the band near 2200 cm^{-1} connected with the C–D stretching in CH_3D with high resolution. At the time when this investigation had been started, in 1956, REA and THOMPSON[4] published normal vibration frequencies of CHD_3 obtained from infrared measurements. The assignments of two of the fundamental bands as well as the frequency value of one more fundamental are, however, in disagreement with infrared results of WILMSHURST and BERNSTEIN[5] (1957). The latter authors have published fundamental frequencies of all the deuterated methanes obtained with low resolution, the frequency values being the position of maximum intensity in the bands rather than the true band centre frequencies.

Recently JONES[6] (1960) has published the results of an infrared study of the degenerate C–H stretching fundamental of CH_3D at 3016 cm^{-1} using medium resolution (≈ 1 cm^{-1}). Only the central part and the high frequency side of the band were measured. Some of his band constants deviate somewhat from the results of a recent Raman investigation of this band by RICHARDSON et al.[7]

The present paper will deal only with CH_3D. Similar results obtained for CH_2D_2 and CHD_3 will be given in separate papers.

II. Experimental

1. Preparations

CH_3D was prepared from CH_3I by allowing the halogen compound to react with a mixture of Zn-dust, acetic anhydride, and heavy water (99.83 % D_2O) at about 30° C. The methyl iodide was carefully distilled before use. The Zn-dust and acetic anhydride were of the highest purity commercially available. The acetic anhydride was carefully distilled and kept for a few days over metallic sodium in order to remove a small content of acetic acid.

The reaction was carried out by adding the methyl iodide dropwise to the mixture of Zn-dust, acetic anhydride, and D_2O (vigorous reaction!). The CH_3D evolved was collected in a gasometer and from there passed through a dry ice trap and then condensed in a liquid air trap. A volume of the gas first collected, equal to the volume of the reaction vessel, was rejected, as it would mainly consist of air. The CH_3D was then distilled *in vacuo* to another liquid air trap. This procedure was repeated once more. In this way the deutero-methane was separated from less volatile impurities (e.g. H_2O from the gasometer).

In a similar way CH_2D_2 and CHD_3 can be prepared from respectively CH_2I_2 and $CHCl_3$.

It follows from the method of preparation that the deutero-methanes will be contaminated by some D_2 and air. These contaminants were removed by successively pumping off small fractions of deutero-methane kept in a liquid air trap until an equilibrium pressure of 20–25 mm Hg was obtained.

In each sample the only spectroscopically detectable impurity was the nearest lower deuterated methane, the amount of this, about 5 per cent., being spectrally of little significance. Table 1 gives the results from the preparations.

Table 1. Results of preparations.

Deuterated compound	Mol halogen compound	Gram atom Zn	Mol $(CH_3CO)_2O$	Mol D_2O	Yield Litre and %
CH_3D	0.29 (CH_3I)	1.26	0.54	3.75	3.5 (50)
CH_2D_2	0.21 (CH_2I_2)	1.33	1.00	2.50	3.7 (73)
CHD_3	0.05 (CHI_3)	0.21	0.13	3.10	0.36 (30)

2. Spectroscopic Procedure

The spectra were taken on a slightly modified Beckman IR3 infrared spectrometer equipped with KBr, NaCl, and LiF prisms.[8] The path length could be varied from 10 to 2000 cm. The effective slit width, s_{eff},[9] is indicated at each spectrum reproduced below together with values of the gas pressure in mm Hg (p) and the path length in cm (l).

The relative positions of the fine structure components within a single band are believed to be accurate within $\pm 0.1-0.2$ cm^{-1}. The absolute accuracy of the frequencies given is estimated at about ± 0.5 cm^{-1}. All the frequencies are in cm^{-1}.

III. Fundamental Bands

The molecule CH_3D is a symmetric top belonging to the point group C_{3v} and therefore has 6 normal vibrations: 3 totally symmetric of species A_1 and 3 doubly degenerate of species E. They are all infrared active. The A_1 vibrations give rise to parallel bands while the E vibrations appear in the spectrum as perpendicular bands.

1. Parallel Bands (A_1 Fundamentals)

The parallel bands corresponding to the vibrations ν_{4a}, ν_{3a}, and ν_1 lie in the regions 1200–1400 cm^{-1}, 2050–2300 cm^{-1}, and 2900–3000 cm^{-1} with observed band centres at 1306, 2200, and 2970 cm^{-1}, respectively. The J fine structure of the P and R branches was easily resolved because of the high value of the rotational constant B'' (≈ 3.9 cm^{-1}), the spacing in the branches being roughly $2B''$.

On the low frequency side, the ν_{4a} band at 1306 cm^{-1} is overlapped by the strong perpendicular band, ν_{4bc}, at 1157 cm^{-1}, and on the high frequency side by the weak perpendicular band, ν_{2ab}, at 1471 cm^{-1}. Furthermore, fine structure components from the strong band $\nu_4(F_2)$ of CH_4, the band centre of which nearly coincides with ν_{4a} of CH_3D, were present in the spectrum indicating a small content of CH_4 in the CH_3D sample. However, because of the high intensity of the ν_{4a} band, assignment of P and R lines up to $J = 11$ could be made quite easily.

The 2200 cm^{-1} band (ν_{3a}) has been analyzed by Boyd and Thompson,[2] and recently by Allen and Plyler.[3] The author's measurements of the

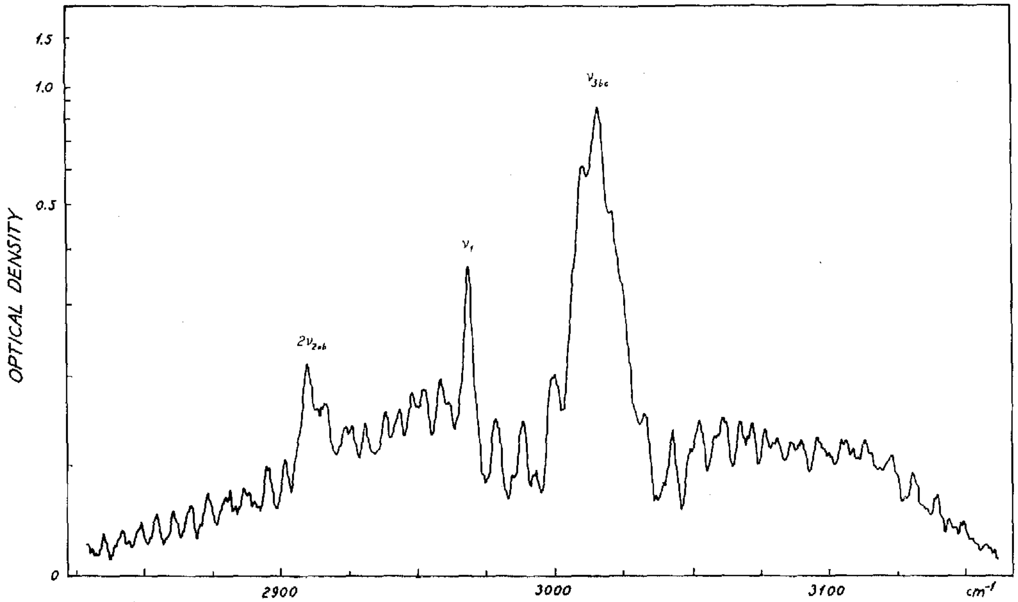

Fig. 1. $\nu_1(A_1)$ and $\nu_{3\,bc}(E)$. 2830–3170 cm^{-1}. $p = 93$ mm. $l = 10$ cm. $s_{\text{eff}} = 2.1$–2.3 cm^{-1}.

same band are in good agreement with their results in spite of the lower resolving power of the IR 3 instrument. In this way a satisfactory check on the spectroscopic procedure used in the present investigation was obtained.

The high intensity of the nearby overtone $2\nu_{4\,bc}$ ($2 \times 1157 = 2314$ cm^{-1}) observed at 2316 cm^{-1} indicates a Fermi resonance between the A_1 component of this overtone and $\nu_{3\,a}$. I have estimated the unperturbed frequency of $\nu_{3\,a}$ at 2210 ± 5 cm^{-1}.

Also ν_1 (Figs. 1 and 4) appears in the spectrum as one of the components of a doublet caused by Fermi resonance with the A_1 part of the overtone $2\nu_{2\,ab}$ ($2 \times 1471 = 2942$ cm^{-1}). The components are observed at 2970 and 2910 cm^{-1}, Wilmshurst and Bernstein found 2973 and 2914 cm^{-1}. If we assume that the anharmonicity of the overtone $2\nu_{2\,ab}$ is -10 cm^{-1}—as seems reasonable—then the unperturbed level ν_1 has been raised 22 cm^{-1}, which means that the unperturbed frequency of ν_1 is close to $2970 - 22 = 2948$ cm^{-1}. As the most probable value, $\nu_1 = 2948 \pm 5$ cm^{-1} has been adopted (see note added in proof, p. 34).

Since the observed band at 2970 cm^{-1} is of low intensity and badly overlapped by the strong perpendicular band, $\nu_{3\,bc}$, at 3016 cm^{-1}, the assignment of the P and R lines is rather uncertain and must be regarded as tentative only.

The analysis of the rotational structure has been carried out by means of the well-known "method of combination differences". Neglecting the effect of centrifugal distortion, the P and R branches can be represented by

$$P(J) = \nu_0 - (B' + B'')J + (B' - B'')J^2 \quad (1)$$

and

$$R(J) = \nu_0 + 2B' + (3B' - B'')J + (B' - B'')J^2. \quad (2)$$

Double-primed quantities refer to the vibrational ground state, single-primed constants to vibrationally excited levels. The combination relations are:

$$R(J-1) + P(J) = 2\nu_0 + 2(B' - B'')J^2 \quad (3)$$

$$\Delta_2 F''(J) = R(J-1) - P(J+1) = 4B''(J+1/2) \quad (4)$$

and

$$\Delta_2 F'(J) = R(J) - P(J) = 4B'(J+1/2). \quad (5)$$

If we take centrifugal distortion into account, D_J'' and D_J' being the centrifugal distortion coefficients, the following relations hold:

$$R(J-1) + P(J) = 2\nu_0 + 2(B' - B'')J^2 - 2(D_J' - D_J'')J^2(J^2+1) \quad (6)$$

$$\Delta_2 F''(J) = 4B''(J+1/2) - 8D_J''(J+1/2)^3 \quad (7)$$

and

$$\Delta_2 F'(J) = 4B'(J+1/2) - 8D_J'(J+1/2)^3. \quad (8)$$

The difference between D_J' and D_J'' can be ignored. Eq. (6) then becomes identical with Eq. (3). Eqs. (7) and (8) can be rewritten

$$\frac{\Delta_2 F''(J)}{J+1/2} = 4B'' - 8D_J''(J+1/2)^2 \quad (9)$$

and

$$\frac{\Delta_2 F'(J)}{J+1/2} = 4B' - 8D_J'(J+1/2)^2. \quad (10)$$

Graphical representation of Eqs. (3)–(5) and (9) and (10) give the band-centre frequencies ν_0, the rotational constants B'' and B', and the difference B'–B''. The results are summarized in Table 2. Only for the ν_{3a} band, values (approximate) of D_J'' and D_J' could be obtained. For this band the results agree well with the results of the high resolution study by Allen and Plyler. The observed frequencies of the fine structure components have therefore been omitted. Observed frequencies and their interpretation for two of the bands (ν_1 and ν_{4a}), together with calculated frequency values, are given in Tables 3 and 4. The agreement appears to be satisfactory.

Table 2. Band constants obtained for parallel bands.

	ν_1* cm^{-1}	ν_{3a}** cm^{-1}	ν_{4a} cm^{-1}
ν_0***	2970.1 ± 0.5	2200.0 ± 0.5 (2200.03)	1306.5 ± 0.5
$B' - B''$	-0.02 ± 0.02	-0.040 ± 0.002 (-0.0422)	-0.088 ± 0.002
B''	3.90 ± 0.02	3.875 ± 0.005 (3.880_0)	3.89 ± 0.01
B'..........	3.92 ± 0.04	3.835 ± 0.005 (3.837_8)	3.80 ± 0.01
D_J''	—	$4._4 \times 10^{-5}$ (5×10^{-5})	—
D_J'	—	$4._4 \times 10^{-5}$ ($5._5 \times 10^{-5}$)	—

* High frequency component of a Fermi doublet. The unperturbed value of ν_1 is close to 2948 cm^{-1} (see text).

** The values in brackets are those obtained by ALLEN and PLYLER[3] (see text).

*** In Table 14 of this paper ν_0 values obtained by other investigators are compared to the author's.

Table 3. Observed and calculated fine structure lines of $\nu_1\,(A_1)$ band.

$P(J)$				$R(J)$			
J	Obs. cm^{-1}	Calc. cm^{-1}	Δ Calc.-obs.	J	Obs. cm^{-1}	Calc. cm^{-1}	Δ Calc.-obs.
				0	2978.3	2977.9	-0.4
1	2962.1	2962.3	0.2	1	2985.7	2985.6	-0.1
2	2954,0	2954.5	0.5	2	2993.5	2993.3	-0.2
3	2946,4	2946,6	0.2	3	3001.0	3000.9	-0.1
4	2938.5	2938.7	0.2	4	3009.0	3008.5	-0.5
5	2931.1	2930.7	-0.4				
6	2923.3	2922.7	-0.6				
7	2914.0	2914.7	0.7				
8	2906.7	2906.6	-0.1				

Effective slit width $s_{\text{eff}} = 1.3\text{–}1.4$ cm^{-1}.

2. Perpendicular Bands (*E* Fundamentals)

The perpendicular bands arising from the normal vibrations ν_{2ab}, ν_{3bc}, and ν_{4bc} are, as already mentioned, observed at 1471, 3016, and 1157 cm^{-1} (Figs. 1, 2, 3, 4, and 5). The K fine structure was resolved for all three bands. The average Q line spacings $\Delta\nu_{2ab}$ and $\Delta\nu_{3bc}$ were found to have approximately the numerical values 5.8 cm^{-1}, respectively 1.9 cm^{-1}. Each of the spacings can be either 'positive' or 'negative'. If the Q line spacing of a band is 'negative', it implies that the ${}^RQ_K$ lines occur on the *low* frequency

Table 4. Observed and calculated fine structure lines of $\nu_{4a}(A_1)$ band.

$P(J)$				$R(J)$			
J	Obs. cm^{-1}	Calc. cm^{-1}	Δ Calc.-obs.	J	Obs. cm^{-1}	Calc. cm^{-1}	Δ Calc.-obs.
				0	1313.7	1314.1	0.4
1	—	1298.7	—	1	1320.9	1321.5	0.6
2	1290.2	1290.8	0.6	2	1328.0	1328.8	0.8
3	1282.3	1282.6	0.3	3	1335.8	1335.9	0.1
4	1274.4	1274.3	−0.1	4	1342.3	1342.8	0.5
5	1265.8	1265.9	0.1	5	1349.5	1349.5	0.0
6	1257.6	1257.2	−0.4	6	1356.0	1356.1	0.1
7	1248.3	1248.4	0.1	7	1362.4	1362.4	0.0
8	1239.5	1239.4	−0.1	8	1368.6	1368.7	0.1
9	1230.0	1230.2	0.2	9	1374.6	1374.7	0.1
10	1220.8	1220.8	0.0	10	1380.7	1380.5	−0.2
11	1211.1	1211.3	0.2	11	1386.5	1386.2	−0.3

Effective slit width $s_{eff} = 1.8\text{–}2.4\ cm^{-1}$.

side of the band centre. For ν_{3bc} the sign of the spacings can be established in the following way. Using the approximate formula for the Coriolis coupling coefficient given by MEAL and POLO[10]

$$\zeta_{3bc} = \frac{(1-\cos\alpha)\, m_H}{m_C + (1-\cos\alpha)\, m_H},$$

we find $\zeta_{3bc} = 0.10$. From the value of ζ_{3bc} we can calculate an approximate value for $\Delta\nu_{3bc}$. The average spacing, $\Delta\nu_i$, in a perpendicular band corresponding to the vibration ν_i is equal to $2\,[A_i'(1-\zeta_i) - B_i']$. Setting $A_{3bc}' \simeq A'' = 5.25\ cm^{-1}$ (see page 30) and $B_{3bc}' \simeq B'' = 3.88\ cm^{-1}$ (see Table 2), we obtain $\Delta\nu_{3bc} = 1.7\ cm^{-1}$, which is close to the observed value. This shows that the sign of $\Delta\nu_{3bc}$ is positive.

The question whether $\Delta\nu_{2ab}$ is positive or negative is connected with the magnitude of the spacing in the third perpendicular band ν_{4bc}. To a good approximation the average Q line spacings of the perpendicular bands will obey the sum rule[11]

$$\Delta\nu_{2ab} + \Delta\nu_{3bc} + \Delta\nu_{4bc} \simeq 6\,A'' - 7\,B'' = 4.34\ cm^{-1},$$

where $A'' = 5.25\ cm^{-1}$ and $B'' = 3.88\ cm^{-1}$. From the relation it follows that at least one of the bands must have a 'negative' spacing, which means that $\zeta_i > 1 - B_i'/A_i' \simeq 1 - B''/A'' = 0.26$. Setting $\Delta\nu_{2ab} = +5.8\ cm^{-1}$ and $\Delta\nu_{3bc} =$

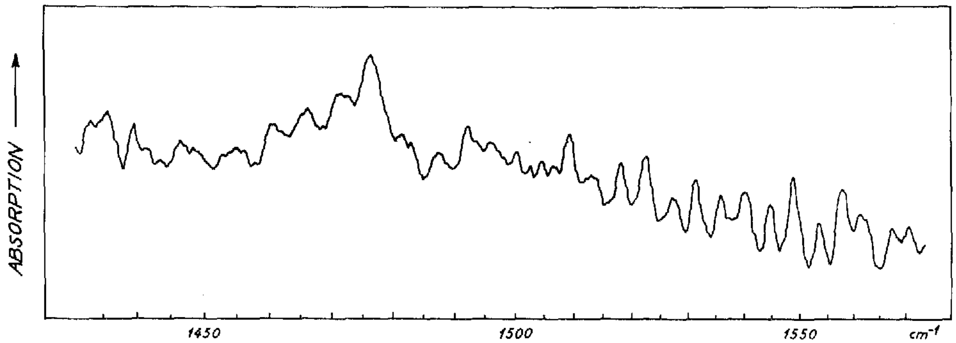

Fig. 2. $\nu_{2ab}(E)$. 1430–1570 cm^{-1}. p = 760 mm. l = 10 cm. s_{eff} = 2.0–2.5 cm^{-1}.

$+1.9$ cm^{-1} in the sum rule, one obtains $\Delta\nu_{4bc} = -3.4$ cm^{-1}, while $\Delta\nu_{2ab} = -5.8$ cm^{-1} and $\Delta\nu_{3bc} = +1.9$ cm^{-1} gives $\Delta\nu_{4bc} = +8.2$ cm^{-1}. For $|\Delta\nu_{4bc}|$ the value 3.4 cm^{-1} is found experimentally. Consequently, the spacings of the ν_{2ab} and ν_{4bc} bands must be respectively 'positive' and 'negative'.

This result is also supported by the observed relative intensities of the Q branches near the two band centres. As $^RQ_0$ is the strongest of the Q lines, and $^PQ_1$ is stronger than $^RQ_1$, the spacing in the ν_{2ab} band (see Fig. 2) should be positive. In the ν_{4bc} band (see Fig. 5) it follows from the same kind of argument that the spacing is negative.

The rotational analysis of the bands is based on the preceding discussion.

A characteristic feature of all three perpendicular bands is the strong central part caused by an agglomeration of the Q lines near the band centre, and the complicated fine structure, consisting of ^PQ_K, ^RQ_K, $^PP_K(J)$, and $^RR_K(J)$ lines and the much weaker $^PR_K(J)$ and $^RP_K(J)$ lines. The K numbering of the Q lines was carried out in the usual way, and the observed frequencies are shown in Tables 8, 9, and 10. The assignments were to some extent complicated by the limited resolving power of the instrument and the overlapping by other bands.

On the high frequency side of the band ν_{4bc} some of the fine structure lines are masked by the strong band at 1306 cm^{-1}. The low frequency side of the weak band ν_{2ab} is overlapped by the absorption at 1306 cm^{-1}. For this reason, only a few ^PQ_K lines and one $^PP_K(J)$ line could be picked out of this band. On the other hand, the high frequency side of the band seems to be free from overlapping by other bands and has therefore been used for the evaluation of the band constants as discussed below. In the band ν_{3bc} there is an overlapping on the long wave side by the weak parallel band

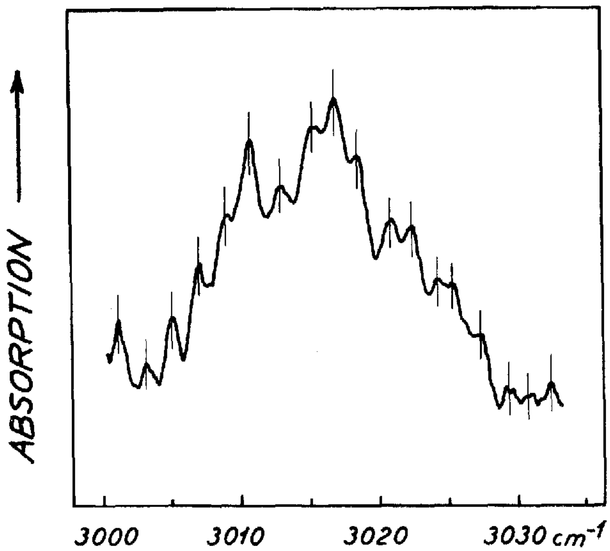

Fig. 3. $\nu_{3\,bc}(E)$. 3000–3030 cm^{-1}. $p = 65$ mm. $l = 10$ cm. $s_{eff} = 1.4$ cm^{-1}.

at 2970 cm^{-1}. However, from the fine structure analysis band constants could be obtained which gave satisfactory agreement between calculated and observed frequencies.

The positions of the Q branches of a perpendicular band, neglecting centrifugal distortion, are given by

$$\left.\begin{aligned} {}^{P}Q_K(J) &= [\nu_0 + A_i'(1-\zeta_i)^2 - B_i'] + (B_i' - B'')\,J(J+1) \\ &\quad - 2\,[A_i'(1-\zeta_i) - B_i']\,K + [(A_i' - A'') - (B_i' - B'')]\,K^2 \end{aligned}\right\} \tag{11}$$

and

$$\left.\begin{aligned} {}^{R}Q_K(J) &= [\nu_0 + A_i'(1-\zeta_i)^2 - B_i'] + (B_i' - B'')\,J(J+1) \\ &\quad + 2\,[A_i'(1-\zeta_i) - B_i']\,K + [(A_i' - A'') - (B_i' - B'')]\,K^2. \end{aligned}\right\} \tag{12}$$

Disregarding the difference between B_i' and B'' the following combination relations can be obtained:

$$\Delta_2 F''(J, K) = {}^{R}Q_{K-1} - {}^{P}Q_{K+1} = 4\,[A'' - A_i'\zeta_i - B'']\,K \tag{13}$$

$$\Delta_2 F'(J, K) = {}^{R}Q_K - {}^{P}Q_K = 4\,[A'(1-\zeta_i) - B_i']\,K \tag{14}$$

$${}^{R}Q_K + {}^{P}Q_K = 2\,[\nu_0 + A_i'(1-\zeta_i)^2 - B_i'] + 2\,[(A_i' - A'') - (B_i' - B'')]\,K^2. \tag{15}$$

Plotting these expressions for the bands $\nu_{3\,bc}$ and $\nu_{4\,bc}$, we obtain the values of the band constants given in Table 5.

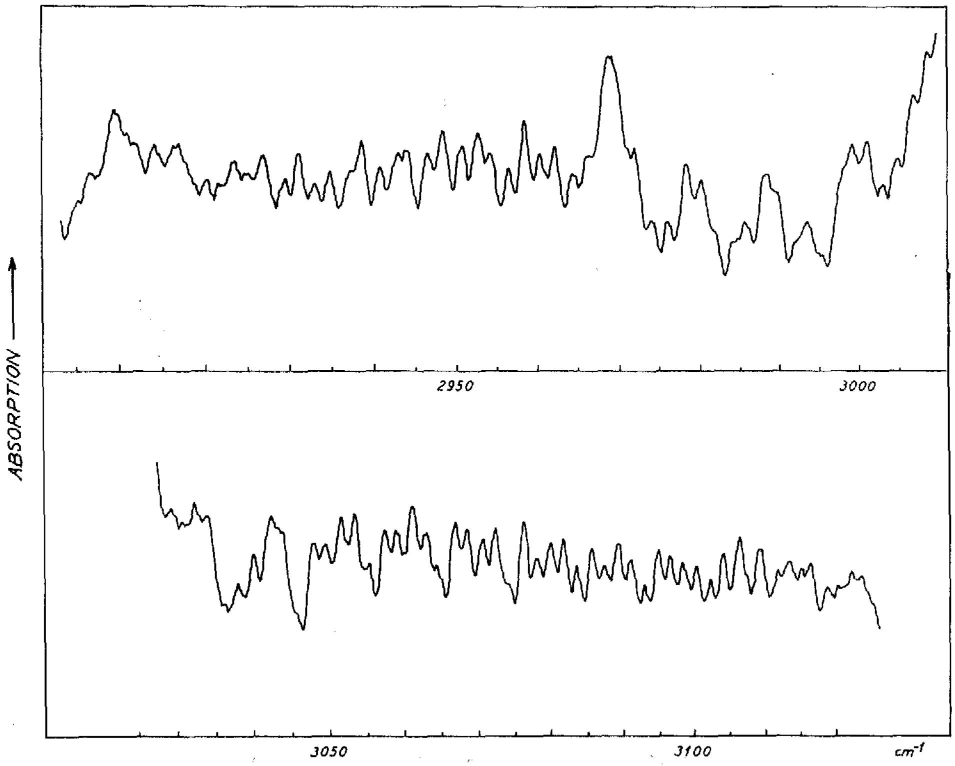

Fig. 4. $\nu_1(A_1)$ and $\nu_{3\,bc}(E)$. Upper curve: 2905–3010 cm^{-1}. Lower curve: 3030–3125 cm^{-1}. $p = 152$ mm. $l = 10$ cm. $s_{\text{eff}} = 1.3$–1.5 cm^{-1}.

Table 5. Preliminary values of band constants for perpendicular bands.

	$\nu_{2\,ab}$ cm^{-1}	$\nu_{3\,bc}$ cm^{-1}	$\nu_{4\,bc}$ cm^{-1}
$A'_i(1-\zeta_i)-B'_i$	2.91 ± 0.03	0.944 ± 0.005	−1.69 ± 0.02
$A''-A'_i\zeta_i-B''$	(2.95)	0.954 ± 0.005	−1.68 ± 0.01
$(A'_i-A'')-(B'_i-B'')$	−0.040 ± 0.01	−0.011 ± 0.003	0.013 ± 0.003
$\nu_0+A'_i(1-\zeta_i)^2-B'_i$	1476.1 ± 0.5	3016.8 ± 0.5	1154.6 ± 0.5

As only two ${}^PQ_K$ lines of the band $\nu_{2\,ab}$ could be utilized, another procedure was attempted. From the observed values of ${}^PQ_5$, ${}^PQ_6$, ${}^RQ_5$, and ${}^RQ_6$ we calculate for $A'_{2\,ab}(1-\zeta_{2\,ab})-B'_{2\,ab}$ from Eq. (14) the values 2.905 cm^{-1} and 2.913 cm^{-1}, the average value being 2.91 cm^{-1}.

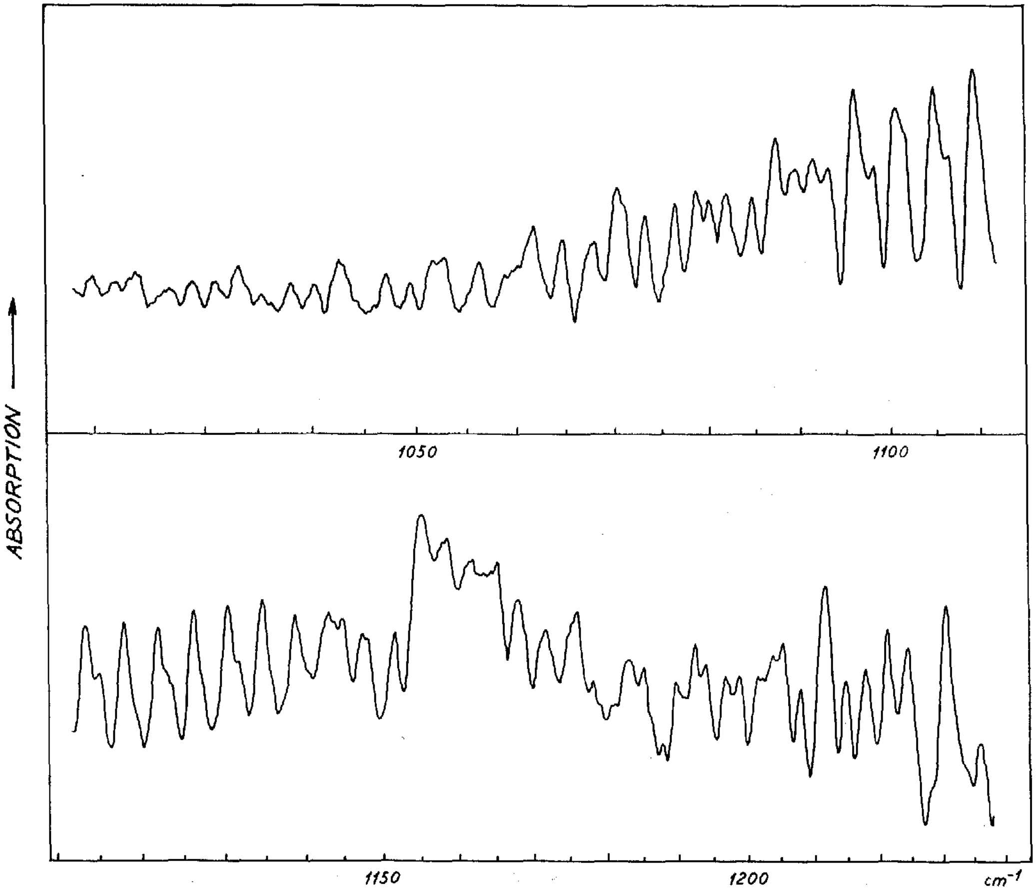

Fig. 5. $\nu_{4\,bc}(E)$. Upper curve: 1020–1110 cm^{-1}. $p = 760$ mm. Lower curve: 1110–1235 cm^{-1}. $p = 323$ mm. $l = 10$ cm. $s_{\text{eff}} = 1.3$–1.9 cm^{-1}.

In order to get a rough estimate of $(A'_{2\,ab} - A'') - (B'_{2\,ab} - B'')$, Eq. (15) was used. Taking the observed $^RQ_0 = 1476.3 = \nu_0 + A'_{2\,ab}(1 - \zeta_{2\,ab})^2 - B'_{2\,ab}$, and using the observed frequencies of $^PQ_5$, $^PQ_6$, $^RQ_5$, and $^RQ_6$, we obtain the values -0.03 and -0.05 cm^{-1}, the average being -0.04 cm^{-1}.

In order to make use of the observed ^RQ_K lines, Eq. (12) was written in the form

$$^RQ_K - 2\,[A'_{2\,ab}(1 - \zeta_{2\,ab}) - B'_{2\,ab}]\,K = [\nu_0 + A'_{2\,ab}(1 - \zeta_{2\,ab})^2 - B'_{2\,ab}] + [(A'_{2\,ab} - A'') - (B'_{2\,ab} - B'')]\,K^2,$$

neglecting the term $(B'_{2ab}-B'')J(J+1)$. From a plot of this expression, where $A'_{2ab}(1-\zeta_{2ab})-B'_{2ab} = 2.91$ cm^{-1}, we obtain

$$\nu_0 + A'_{2ab}(1-\zeta_{2ab})^2 - B'_{2ab} = 1476.1 \text{ cm}^{-1}$$

and

$$(A'_{2ab}-A'')-(B'_{2ab}-B'') = -0.040 \text{ cm}^{-1}$$

in good agreement with the values above.

The assignment of the $^PP_K(J)$ and $^RR_K(J)$ lines of the three bands was carried out in the following way.

The positions of the $^PP_K(J)$ and $^RR_K(J)$ lines are given by the equations

$$^PP_K(J) = {^PQ_K}(J) - 2B'_iJ + 4D_JJ^3 \tag{16}$$

and

$$^RR_K(J) = {^RQ_K}(J) + 2B'(J+1) - 4D_J(J+1)^3, \tag{17}$$

where the following approximations have been made: $D''_J = D'_J = D_J$, $D''_{JK} = D'_{JK} = 0$ and $D''_K = D'_K = 0$. It should, however, be emphasized that for higher J and K values, i.e. $J \geq 10$ and $K \geq 6$, approximately, it may not be permissible to ignore the D_{JK} and D_K terms. The D_{JK} and D_K values found by Richardson *et al.* for the ν_{3bc} band show this.

In order to calculate approximate values for the $^PP_K(J)$ and $^RR_K(J)$ lines of the three bands, Eqs. (16) and (17) were used together with Eqs. (11) and (12), the band constants given in Table 5 being inserted, and $B'_i = B'' = 3.88$ cm^{-1}. D_J was taken to 5.5×10^{-5} cm^{-1}, which is close to the value of D'_J and D''_J for ν_{3a} obtained by Boyd and Thompson[2] and Allen and Plyler.[3] Then, calculating the relative intensities of the transitions from the formulae quoted by Herzberg,[12] taking $B'' = 3.880$ cm^{-1} and $A'' = 5.245$ cm^{-1} (see page 30), it was possible to pick out a number of $^PP_3(J)$ and $^RR_3(J)$ lines in the ν_{3bc} and ν_{4bc} bands. For the analysis, the following combination relations were used:

$$\left.\begin{aligned} {^RR_K}(J) - {^PP_K}(J) &= 4\,[A'_i(1-\zeta_i)-B'_i]\,K + 4'_i B\,(J+1/2) \\ &\quad - 4D_J[(J+1)^3+J^3] \end{aligned}\right\} \tag{18}$$

$$\left.\begin{aligned} {^RR_K}(J-1) - {^PP_K}(J+1) &= 4[A'_i(1-\zeta_i)-B'_i]\,K + 4B''(J+1/2) \\ &\quad - 4D_J[J^3+(J+1)^3] \end{aligned}\right\} \tag{19}$$

$$\left.\begin{aligned} {^RR_K}(J-1) + {^PP_K}(J) &= 2\,[\nu_0 + A'_i(1-\zeta_i)^2 - B'_i] \\ &\quad + 2\,[(A'_i-A'')-(B'_i-B'')]\,K^2 + 2\,(B'_i-B'')\,J^2, \end{aligned}\right\} \tag{20}$$

where $K = 3$. The small term $4D_J[J^3-(J-1)^3]$ has been omitted. Using the values of $A'_i(1-\zeta_i)-B'_i$ and $(A'_i-A'')-(B'_i-B'')$ from Table 5, and $D_J = 5.5\times10^{-5}$ cm^{-1}, graphical representations of Eqs. (18), (19), and (20) gave

Table 6. Preliminary values of band constants for $\nu_{3\,bc}$ and $\nu_{4\,bc}$ bands.

	$\nu_{3\,bc}$ cm^{-1}	$\nu_{4\,bc}$ cm^{-1}
B'	3.873 ± 0.005	3.86 ± 0.01
B''	3.882 ± 0.005	3.88 ± 0.01
$B'-B''$	-0.011 ± 0.002	-0.013 ± 0.005
$\nu_0 + A_i'(1-\zeta_i)^2 - B_i'$	3016.9 ± 0.5	1154.7 ± 0.5
D_J	$5._5 \times 10^{-5}$	—

the values of B_i', B'', $B_i'-B''$, and $\nu_0 + A_i'(1-\zeta_i)^2 - B_i'$, listed in Table 6. For the $\nu_{3\,bc}$ band, it was possible to obtain a value of D_J. Using the approximation $J^3 + (J+1)^3 \simeq 2(J+1/2)^3$, Eqs. (18) and (19) were written:

$$\frac{{}^RR_3(J) - {}^PP_3(J) - 12\,[A_i'(1-\zeta_i) - B_i']}{J+1/2} = 4\,B_i' - 8\,D_J\,(J+1/2)^2 \tag{21}$$

and

$$\frac{{}^RR_3(J-1) - {}^PP_3(J+1) - 12\,[A_i'(1-\zeta_i) - B_i']}{J+1/2} = 4\,B'' - 8\,D_J\,(J+1/2)^2. \tag{22}$$

Graphical representations gave B_i', B'', and D_J (5×10^{-5} and $6 \times 10^{-5}\ \mathrm{cm}^{-1}$, see Table 6).

For the $\nu_{2\,ab}$ band, it was assumed that $B_i' - B'' = -0.015\ \mathrm{cm}^{-1}$, which then gives $B_i' = 3.865\ \mathrm{cm}^{-1}$.

Table 7 shows the final values of the band constants used for calculating the frequencies in Tables 8, 9, and 10. As will be seen, some of the band constants have been slightly adjusted in order to improve the agreement between observed and calculated frequencies.

It has been possible to explain nearly all the observed lines as ${}^PQ_K$, ${}^RQ_K$, ${}^PP_K(J)$, and ${}^RR_K(J)$ lines. Only a few lines had to be interpreted as ${}^PR_K(J)$ and ${}^RP_K(J)$ lines. Although ${}^PR_K(J)$ and ${}^RP_K(J)$ lines generally contribute to the intensities of the observed lines, it was thought permissible to omit them in most cases because of their low intensity and the limited resolving power of the instrument. ${}^RP_K(J)$ lines have, however, had to be included in the *low* frequency region of the $\nu_{4\,bc}$ band in order to get reasonable agreement between observed and calculated intensities.

The frequencies of the ${}^RP_K(J)$ and ${}^PR_K(J)$ lines were calculated from the expressions

$${}^RP_K(J) = {}^RQ_K(J) - 2\,B_i'J + 4\,D_J J^3 \tag{23}$$

$${}^PR_K(J) = {}^PQ_K(J) + 2\,B_i'(J+1) - 4\,D_J\,(J+1)^3. \tag{24}$$

Table 7. Finally adopted values of band constants for perpendicular bands.

	$\nu_{2\,ab}$ cm^{-1}	$\nu_{3\,bc}$ cm^{-1}	$\nu_{4\,bc}$ cm^{-1}
$\nu_0 + A_i'(1-\zeta_i)^2 - B_i'$	1476.1	3016.8	1154.7
$A_i'(1-\zeta_i) - B_i'$	2.91	0.944	−1.70
$(A_i' - A'') - (B_i' - B'')$	−0.040	−0.011	0.013
B''	3.880	3.880	3.880
B_i'	3.865	3.869	3.865
$B_i' - B''$	−0.015	−0.011	−0.015
D_J	5.5×10^{-5}	5.5×10^{-5}	5.5×10^{-5}

For higher K and J values, deviations between observed and calculated frequencies can be expected due to the neglect of the D_{JK} and D_K terms in Eqs. (16) and (17). In those cases the assignments must be regarded as tentative, although they are often supported by the observed relative intensities of the lines (see Table 10). The relative intensities have been calculated by the author for the $^PP_K(J)$, $^RR_K(J)$, $^RP_K(J)$, and $^PR_K(J)$ lines. For the $\nu_{2\,ab}$ and $\nu_{4\,bc}$ bands, the relative intensities of the Q lines will not deviate much from the corresponding Q line intensities of the $\nu_{3\,bc}$ band, calculated by JONES.[6]

Table 8. Observed and calculated fine structure lines of $\nu_{2\,ab}\,(E)$ band.

Obs. cm^{-1}	Assignment	Calc. cm^{-1}	Δ (Calc.-obs.)	Calc. relative intensity
1432.8[a]	$^PP_1(5)$	1431.1	−1.7	3.1
	$^PP_2(4)$	1433.1	0.3	4.6
1435.4	$^PP_3(3)$	1434.9	−0.5	14.0
1439.5	$^PQ_6$	1439.7	0.2	
	$^PP_1(4)$	1439.0	−0.5	3.1
1441.5[a]	$^PP_2(3)$	1440.9	−0.6	4.8
1446.4	$^PQ_5$	1446.0	−0.4	
	$^PP_1(3)$	1446.8	0.4	2.9
1448.3[a]	$^PP_2(2)$	1448.8	0.5	4.8
1453.0[a]	$^PQ_4$	1452.2	−0.8	
1455.0[a]	$^PP_1(2)$	1454.7	−0.3	2.5
1460.7	$^PQ_3$	1458.3	−2.4	
	$^PP_1(1)$	1462.4	1.7	1.8
1465.8	$^PQ_2$	1464.3	−1.5	

(To be continued)

Table 8 (continued).

Obs. cm^{-1}	Assignment	Calc. cm^{-1}	Δ (Calc.-obs.)	Calc. relative intensity
1471.3	${}^{P}Q_1$	1470.2	−1.1	
1476.3	${}^{R}Q_0$	1476.1	−0.2	
1481.8	${}^{R}Q_1$	1481.9	0.1	
1482.9[a]	${}^{R}R_0\,(0)$	1483.8	0.9	3.8
1487.4	${}^{R}Q_2$	1487.6	0.2	
1492.1	${}^{R}R_0\,(1)$	1491.5	−0.6	5.5
1493.0[a]	${}^{R}Q_3$	1493.2	0.2	
1496.0	${}^{R}R_1\,(1)$	1497.3	1.3	5.5
1498.0[a]	${}^{R}Q_4$	1498.8	0.8	
1500.2	${}^{R}R_0\,(2)$	1499.2	−1.0	6.9
1504.5	${}^{R}Q_5$	1504.2	−0.3	
	${}^{R}R_1\,(2)$	1505.0	0.5	5.7
1506.2	${}^{R}R_0\,(2)$	1506.8	0.6	7.7
1509.4	${}^{R}Q_6$	1509.6	0.2	
	${}^{R}R_2\,(2)$	1510.7	1.3	8.3
1513.1	${}^{R}R_0\,(4)$	1514.3	1.2	8.0
	${}^{R}R_1\,(3)$	1512.6	−0.5	5.7
	${}^{R}Q_7$	1514.8	1.7	
1518.0	${}^{R}R_1\,(4)$	1520.1	2.1	5.6
	${}^{R}R_2\,(3)$	1518.3	0.3	7.9
	${}^{R}Q_8$	1520.0	2.0	
1522.7	${}^{R}R_0\,(5)$	1522.0	−0.7	7.8
	${}^{R}R_3\,(3)$	1523.9	1.2	20.2
1527.3	${}^{R}R_1\,(5)$	1527.8	0.5	5.2
	${}^{R}R_2\,(4)$	1525.9	−1.4	7.3
1531.3	${}^{R}R_0\,(6)$	1529.5	−1.8	7.2
	${}^{R}R_2\,(5)$	1533.5	2.2	6.5
	${}^{R}R_3\,(4)$	1531.5	0.2	18.1
1535.8	${}^{R}R_0\,(7)$	1537.0	1.2	6.3
	${}^{R}R_1\,(6)$	1535.3	−0.5	4.6
	${}^{R}R_4\,(4)$	1537.0	1.2	10.7
1540.2	${}^{R}R_2\,(6)$	1541.0	0.8	5.6
	${}^{R}R_3\,(5)$	1539.1	−1.1	15.7
1544.5	${}^{R}R_0\,(8)$	1544.4	−0.1	5.2
	${}^{R}R_1\,(7)$	1542.8	−1.7	3.9
	${}^{R}R_4\,(5)$	1544.6	0.1	9.1
1548.8	${}^{R}R_1\,(8)$	1550.2	1.4	3.2
	${}^{R}R_2\,(7)$	1548.5	−0.3	4.7
	${}^{R}R_5\,(5)$	1550.1	1.3	10.3
	${}^{R}R_3\,(6)$	1546.6	−2.2	13.2

(To be continued)

Table 8 (continued).

Obs. cm^{-1}	Assignment	Calc. cm^{-1}	Δ (Calc.-obs.)	Calc. relative intensity
1553.5	${}^{R}R_0$ (9)	1551.8	−1.7	4.1
	${}^{R}R_3$ (7)	1554.1	0.6	10.8
	${}^{R}R_4$ (6)	1552.1	−1.4	7.6
1558.0	${}^{R}R_0$ (10)	1559.2	1.2	3.1
	${}^{R}R_1$ (9)	1557.6	−0.4	2.5
	${}^{R}R_2$ (8)	1555.9	−2.1	3.7
	${}^{R}R_4$ (7)	1559.6	1.6	6.1
	${}^{R}R_5$ (6)	1557.6	−0.4	8.4
1561.6	${}^{R}R_2$ (9)	1563.3	1.7	2.8
	${}^{R}R_3$ (8)	1561.5	−0.1	8.5
	${}^{R}R_6$ (6)	1563.0	1.4	18.2
1567.6	${}^{R}R_0$ (11)	1566.5	−1.1	2.2
	${}^{R}R_3$ (9)	1568.9	1.3	6.4
	${}^{R}R_4$ (8)	1567.0	−0.6	4.7
1570.9	${}^{R}R_2$ (10)	1570.8	−0.1	2.1
	${}^{R}R_5$ (8)	1572.5	1.6	5.1
	${}^{R}R_6$ (7)	1570.5	−0.4	14.3

$s_{eff} = 2.0\text{–}2.5$ cm^{-1}.

[a] Not resolved.

Table 9. Observed and calculated fine structure lines of $\nu_{3\,bc}(E)$ band.

Obs. cm^{-1}	Assignment	Calc. cm^{-1}	Δ (Calc.-obs.)	Calc. relative intensity
2914.0	${}^{P}P_4$ (12)	2914.8	0.8	0.9
	P (7) (ν_1)	2914.7	0.7	
2916.6	${}^{P}P_3$ (12)	2916.8	0.2	1.7
	${}^{P}P_7$ (11)	2916.7	0.1	1.6
	${}^{P}P_8$ (11)	2914.7	−1.9	1.6
2920.1	${}^{P}P_1$ (12)	2920.6	0.5	0.6
	${}^{P}P_{10}$ (10)	2918.4	−1.7	1.2
2921.5[a]	${}^{P}P_5$ (11)	2920.8	−0.7	1.5
	${}^{P}P_9$ (10)	2920.5	−1.0	4.7
2923.3	${}^{P}P_4$ (11)	2922.8	−0.5	1.3
	${}^{P}P_8$ (10)	2922.6	−0.7	2.4
	P (6) (ν_1)	2922.7	−0.6	

(To be continued)

Table 9 (continued).

Obs. cm^{-1}	Assignment	Calc. cm^{-1}	Δ (Calc.-obs.)	Calc. relative intensity
2924.8	$^PP_3(11)$	2924.7	−0.1	2.4
	$^PP_7(10)$	2924.6	−0.2	2.3
2927.0	$^PP_2(11)$	2926.7	−0.3	1.1
	$^PP_6(10)$	2926.7	−0.3	4.5
2929.4	$^PP_1(11)$	2928.6	−0.8	0.9
	$^PP_5(10)$	2928.7	−0.7	2.1
	$^PP_9(9)$	2928.4	−1.0	6.9
2931.1	$^PP_4(10)$	2930.7	−0.4	1.9
	$^PP_8(9)$	2930.5	−0.6	3.4
	$P(5)(\nu_1)$	2930.7	−0.4	
2932.8	$^PP_3(10)$	2932.6	−0.2	3.5
	$^PP_7(9)$	2932.5	−0.3	3.3
2934.8	$^PP_2(10)$	2934.6	−0.2	1.5
	$^PP_6(9)$	2934.6	−0.2	6.3
2937.1[a]	$^PP_1(10)$	2936,5	−0.6	1.3
	$^PP_5(9)$	2936.6	−0.5	2.9
2938.5	$^PP_4(9)$	2938.6	0.1	2.7
	$^PP_8(8)$	2938.4	−0.1	4.7
	$P(4)(\nu_1)$	2938.6	0.2	
2940.6	$^PP_3(9)$	2940.5	−0.1	4.8
	$^PP_7(8)$	2940.4	−0.2	4.6
2942.8[a]	$^PP_2(9)$	2942.5	−0.3	2.1
	$^PP_6(8)$	2942.5	−0.3	8.6
2944.2[a]	$^PP_1(9)$	2944.4	0.2	1.7
	$^PP_5(8)$	2944.5	0.3	4.0
2946.4	$^PP_4(8)$	2946.5	0.1	3.6
	$P(3)(\nu_1)$	2946.6	0.2	
2948.2	$^PP_3(8)$	2948.4	0.2	6.2
	$^PP_7(7)$	2948.3	0.1	6.1
2950.6	$^PP_2(8)$	2950.4	−0.2	2.6
	$^PP_6(7)$	2950.4	−0.2	11.4
2952.6	$^PP_1(8)$	2952.3	−0.3	2.2
	$^PP_5(7)$	2952.4	−0.2	5.2
2954.0	$^PP_4(7)$	2954.4	0.4	4.6
	$P(2)(\nu_1)$	2954.5	0.5	
2956.4	$^PP_3(7)$	2956.3	−0.1	7.9
2958.2	$^PP_2(7)$	2958.3	0.1	3.3
	$^PP_6(6)$	2958.2	0.0	14.7

(To be continued)

Table 9 (continued).

Obs. cm^{-1}	Assignment	Calc. cm^{-1}	Δ (Calc.-obs.)	Calc. relative intensity	
2960.2	$^{P}P_1(7)$	2960.2	0.0	2.6	
	$^{P}P_5(6)$	2960.2	0.0	6.6	
2962.1	$^{P}P_4(6)$	2962.2	0.1	5.7	
	$P(1)(\nu_1)$	2962.3	0.2		
2964.4	$^{P}P_3(6)$	2964.2	−0.2	9.6	
2966.0[a]	$^{P}P_2(6)$	2966.1	0.1	3.9	
2971.9	$^{P}P_3(5)$	2972.0	0.1	11.2	
2974.1	$^{P}P_2(5)$	2974.0	−0.1	4.3	
2976.0	$^{P}P_1(5)$	2975.9	−0.1	3.2	
2978.3	$^{P}P_4(4)$	2977.9	−0.4	8.1	
	$R(0)(\nu_1)$	2977.9	−0.4		
2980.2	$^{P}P_3(4)$	2979.8	−0.4	12.7	
2981.7[a]	$^{P}P_2(4)$	2981.8	0.1	4.7	
2984.0[a]	$^{P}P_1(4)$	2983.7	−0.3	3.2	
2985.7	$^{R}P_0(4)$	2985.6	−0.1	3.8	
	$R(1)(\nu_1)$	2985.6	−0.1		
					(Ref. 6)
2988.2	$^{P}P_3(3)$	2987.7	−0.5	14.1	15.1
2989.8[a]	$^{P}P_2(3)$	2989.6	−0.2	4.8	5.2
2991.9[a]	$^{P}P_1(3)$	2991.5	−0.4	3.0	3.2
2993.5	$^{R}P_0(3)$	2993.4	−0.1	3.0	3.2
	$R(2)(\nu_1)$	2993.3	−0.2		
2995.2[a]	$^{P}Q_{11}$	2994.7	−0.5		0.8
	$^{R}P_1(3)$	2995.3	0.1	0.5	0.5
2999.2	$^{P}Q_9$	2998.9	−0.3		5.2
	$^{P}P_1(2)$	2999.4	0.2	2.5	2.7
3001.0	$^{P}Q_8$	3001.0	0.0		4.7
	$R(3)(\nu_1)$	3000.9	−0.1		
3003.1	$^{P}Q_7$	3003.0	−0.1		7.7
3005.0	$^{P}Q_6$	3005.1	0.1		24.5
3007.0	$^{P}Q_5$	3007.1	0.1		18.3
	$^{P}P_1(1)$	3007.1	0.1	1.8	1.9
3009.0[a]	$^{P}Q_4$	3009.1	0.1		26.0
	$R(4)(\nu_1)$	3008.5	−0.5		
3010.6	$^{P}Q_3$	3011.0	0.4		70.0
3012.9	$^{P}Q_2$	3013.0	0.1		44.3
3015.3	$^{P}Q_1$	3014.9	−0.4		52.4
3016.7	$^{R}Q_0$	3016.8	0.1	100	107.5
3018.3	$^{R}Q_1$	3018.7	0.4		45.4
3020.8	$^{R}Q_2$	3020.5	−0.3		36.0

(*To be continued*)

Table 9 (continued).

Obs. cm^{-1}	Assignment	Calc. cm^{-1}	Δ (Calc.-obs.)	Calc. relative intensity	
					(Ref. 6)
3022.3	$^RQ_3$	3022.4	0.1		54.0
3024.2[a]	$^RQ_4$	3024.2	0.0		19.6
	$^RR_0\,(0)$	3024.5	0.3	3.8	4.0
3025.5[a]	$^RQ_5$	3026.0	0.5		13.2
3027.5[a]	$^RQ_6$	3027.7	0.2		17.1
3029.5	$^RQ_7$	3029.5	0.0		5.2
3030.9	$^RQ_8$	3031.2	0.3		3.0
3032.5	$^RQ_9$	3032.9	0.4	3.4	3.4
	$^RR_0\,(1)$	3032.3	−0.2	5.5	5.8
3034.3	$^RQ_{10}$	3034.6	0.3		1.0
	$^RR_1\,(1)$	3034.2	−0.1	5.4	5.8
3036.1[a]	$^RQ_{11}$	3036.2	0.1		0.6
	$^PR_2\,(2)$	3036.1	0.0	0.6	0.6
3037.9	$^PR_1\,(2)$	3038.1	0.2	1.7	1.8
3039.9	$^RR_0\,(2)$	3040.0	0.1	6.8	7.2
3042.2	$^RR_1\,(2)$	3041.9	−0.3	5.6	5.9
3043.7[a]	$^RR_2\,(2)$	3043.7	0.0	8.3	8.7
3045.7[a]	$^PR_1\,(3)$	3045.7	0.0	2.3	2.4
3047.8	$^RR_0\,(3)$	3047.6	−0.2	7.6	8.0
3049.4	$^RR_1\,(3)$	3049.5	0.1	5.7	6.0
3051.4	$^RR_2\,(3)$	3051.3	−0.1	7.8	8.2
3053.3	$^RR_3\,(3)$	3053.2	−0.1	20.1	21.1
3055.4	$^RR_0\,(4)$	3055.3	−0.1	7.9	8.3
3057.4	$^RR_1\,(4)$	3057.2	−0.2	5.5	5.8
3059.0	$^RR_2\,(4)$	3059.0	0.0	7.2	7.5
3061.2	$^RR_3\,(4)$	3060.8	−0.4	17.9	18.7
3062.9	$^RR_0\,(5)$	3062.9	0.0	7.7	8.0
	$^RR_4\,(4)$	3062.7	−0.2	10.7	11.1
3064.4	$^RR_1\,(5)$	3064.8	0.4	5.1	5.3
3066.9	$^RR_2\,(5)$	3066.6	−0.3	6.4	6.7
3068.4	$^RR_3\,(5)$	3068.4	0.0	15.5	16.1
3070.7	$^RR_0\,(6)$	3070.5	−0.2	7.0	7.3
	$^RR_4\,(5)$	3070.3	−0.4	9.1	9.4
3072.3[a]	$^RR_1\,(6)$	3072.4	0.1	4.5	4.7
	$^RR_5\,(5)$	3072.1	−0.2	10.2	10.7
3074.1[a]	$^RR_2\,(6)$	3074.2	0.1	5.5	5.7
3076.3	$^RR_3\,(6)$	3076.0	−0.3	13.0	13.5
3078.2	$^RR_0\,(7)$	3078.0	−0.2	6.1	6.3
	$^RR_4\,(6)$	3077.9	−0.3	7.5	7.7

(To be continued)

Table 9 (continued).

Obs. cm^{-1}	Assignment	Calc. cm^{-1}	Δ (Calc.-obs.)	Calc. relative intensity	(Ref. 6)
3080.1	${}^{R}R_1(7)$	3079.9	−0.2	3.8	3.9
	${}^{R}R_5(6)$	3079.7	−0.4	8.4	10.1
3081.8	${}^{R}R_2(7)$	3081.7	−0.1	4.5	4.7
	${}^{R}R_6(6)$	3081.4	−0.4	18.1	21.8
3083.6	${}^{R}R_3(7)$	3083.6	0.0	10.6	10.9
3085.6	${}^{R}R_0(8)$	3085.5	−0.1	5.1	5.2
	${}^{R}R_4(7)$	3085.4	−0.2	6.0	6.2
3087.4	${}^{R}R_1(8)$	3087.4	0.0	3.1	3.2
	${}^{R}R_5(7)$	3087.2	−0.2	6.6	6.8
3089.4	${}^{R}R_2(8)$	3089.2	−0.2	3.6	3.7
	${}^{R}R_6(7)$	3088.9	−0.5	14.1	14.5
3091.2	${}^{R}R_3(8)$	3091.1	−0.1	8.3	8.5
	${}^{R}R_7(7)$	3090.7	−0.5	7.4	7.6
3093.0	${}^{R}R_0(9)$	3093.0	0.0	4.0	4.1
	${}^{R}R_4(8)$	3092.9	−0.1	4.6	4.7
3095.0	${}^{R}R_1(9)$	3094.9	−0.1	2.4	2.4
	${}^{R}R_5(8)$	3094.7	−0.3	5.0	5.2
3096.8	${}^{R}R_2(9)$	3096.7	−0.1	2.8	2.8
	${}^{R}R_6(8)$	3096.4	−0.4	10.7	10.9
3098.5	${}^{R}R_3(9)$	3098.6	0.1	6.2	6.4
	${}^{R}R_7(8)$	3098.2	−0.3	5.5	5.7
3100.6	${}^{R}R_0(10)$	3100.5	−0.1	3.0	3.1
	${}^{R}R_4(9)$	3100.4	−0.2	3.4	3.5
	${}^{R}R_8(8)$	3099.9	−0.7	5.7	5.8
3102.4	${}^{R}R_1(10)$	3102.4	0.0	1.8	1.8
	${}^{R}R_5(9)$	3102.2	−0.2	3.7	3.8
3104.2	${}^{R}R_2(10)$	3104.2	0.0	2.0	2.1
	${}^{R}R_6(9)$	3103.9	−0.3	7.8	8.0
3106.4	${}^{R}R_3(10)$	3106.0	−0.4	4.5	4.5
	${}^{R}R_7(9)$	3105.7	−0.7	4.0	4.1
3107.4[a]	${}^{R}R_0(11)$	3107.9	0.5	2.2	2.2
	${}^{R}R_4(10)$	3107.9	0.5	2.5	2.5
	${}^{R}R_8(9)$	3107.4	0.0	4.1	4.2
3109.4	${}^{R}R_1(11)$	3109.8	0.4	1.3	1.3
	${}^{R}R_5(10)$	3109.7	0.3	2.6	2.7
	${}^{R}R_9(9)$	3109.1	−0.3	8.1	8.3
3111.9	${}^{R}R_2(11)$	3111.6	−0.3	1.4	1.4
	${}^{R}R_6(10)$	3111.4	−0.5	5.5	5.6

(To be continued)

Table 9 (continued).

Obs. cm^{-1}	Assignment	Calc. cm^{-1}	Δ (Calc.-obs.)	Calc. relative intensity	
					(Ref. 6)
3113.5	$^{R}R_3(11)$	3113.4	−0.1	3.1	3.2
	$^{R}R_7(10)$	3113.2	−0.3	2.8	2.9
3115.3	$^{R}R_0(12)$	3115.3	0.0	1.6	1.5
	$^{R}R_4(11)$	3115.3	0.0	1.7	1.7
	$^{R}R_8(10)$	3114.9	−0.4	2.9	2.9
3116.5	$^{R}R_1(12)$	3117.2	0.7	0.9	0.7
	$^{R}R_5(11)$	3117.1	0.6	1.8	1.9
	$^{R}R_9(10)$	3116.6	0.1	5.6	5.7
3118.9	$^{R}R_2(12)$	3119.0	0.1	1.0	1.0
	$^{R}R_6(11)$	3118.8	−0.1	3.8	4.5

$s_{eff} = 1.3–1.5\ cm^{-1}$.
[a] Not resolved.

Table 10. Observed and calculated fine structure lines of $\nu_{4bc}(E)$ band.

Obs. cm^{-1}	Assignment	Calc. cm^{-1}	Δ (Calc.-obs.)	Calc. relative intensity
1028.6	$^{R}P_2(15)$	1029.2	0.6	0.1
	$^{R}P_0(16)$	1027.8	−0.8	0.2
1030.7	$^{P}P_1(16)$	1031.2	0.5	0.1
	$^{P}P_3(17)$	1030.1	−0.6	0.1
	$^{R}P_4(14)$	1030.5	−0.2	0.1
1033.0	$^{P}P_4(17)$	1033.6	0.6	0.1
	$^{P}P_6(18)$	1031.3	−1.7	0.1
	$^{R}P_1(15)$	1032.5	−0.5	0.1
	$^{R}P_3(14)$	1033.8	0.8	0.3
	$^{R}P_6(13)$	1032.1	−0.9	0.1
1035.0	$^{P}P_2(16)$	1034.7	−0.3	0.1
	$^{R}P_0(15)$	1035.9	0.9	0.3
	$^{R}P_5(13)$	1035.3	0.3	0.1
1037.9	$^{P}P_3(16)$	1038.1	0.2	0.2
	$^{P}P_5(17)$	1037.1	−0.8	0.1
	$^{R}P_2(14)$	1037.2	−0.7	0.2
	$^{R}P_4(13)$	1038.6	0.7	0.1
1040.0	$^{P}P_1(15)$	1039.3	−0.7	0.2
	$^{R}P_1(14)$	1040.5	0.5	0.2
	$^{R}P_6(12)$	1040.1	0.1	0.2

(To be continued)

Table 10 (continued).

Obs. cm^{-1}	Assignment	Calc. cm^{-1}	Δ (Calc.-obs.)	Calc. relative intensity
1042.6	${}^{P}P_{2}(15)$	1042.8	0.2	0.2
	${}^{P}P_{4}(16)$	1041.6	−1.0	0.1
	${}^{P}P_{6}(17)$	1040.7	−1.9	0.1
	${}^{R}P_{0}(14)$	1043.9	1.3	0.4
	${}^{R}P_{3}(13)$	1041.9	−0.7	0.4
	${}^{R}P_{5}(12)$	1043.3	0.7	0.1
1047.1	${}^{P}P_{1}(14)$	1047.3	0.2	0.3
	${}^{P}P_{3}(15)$	1046.2	−0.9	0.4
	${}^{P}P_{5}(16)$	1045.1	−2.0	0.1
	${}^{R}P_{4}(12)$	1046.6	−0.5	0.2
1049.4	${}^{P}P_{4}(15)$	1049.7	0.3	0.2
	${}^{R}P_{1}(13)$	1048.6	−0.8	0.3
1051.4[a]	${}^{P}P_{2}(14)$	1050.8	−0.6	0.3
	${}^{P}P_{6}(16)$	1048.7	−2.4	0.3
	${}^{P}P_{8}(17)$	1047.8	−3.6	0.1
	${}^{R}P_{0}(13)$	1052.0	0.6	0.7
	${}^{R}P_{3}(12)$	1049.9	−1.5	0.5
	${}^{R}P_{5}(11)$	1051.3	−0.1	0.2
1053.0[a]	${}^{P}P_{3}(14)$	1054.2	1.2	0.6
	${}^{P}P_{5}(15)$	1053.2	0.2	0.2
	${}^{P}P_{7}(16)$	1052.2	−0.8	0.1
	${}^{R}P_{2}(12)$	1053.3	0.3	0.3
	${}^{R}P_{4}(11)$	1054.6	1.6	0.3
1056.0	${}^{P}P_{1}(13)$	1055.4	−0.6	0.4
	${}^{P}P_{9}(17)$	1051.5	−4.5	0.1
	${}^{R}P_{1}(12)$	1056.6	0.6	0.4
1059.0[a]	${}^{P}P_{2}(13)$	1058.9	−0.1	0.5
	${}^{P}P_{4}(14)$	1057.7	−1.3	0.3
	${}^{P}P_{6}(15)$	1056.8	−2.2	0.4
	${}^{P}P_{8}(16)$	1055.8	−3.2	0.1
	${}^{R}P_{3}(11)$	1057.9	−1.1	0.7
	${}^{R}P_{5}(10)$	1059.3	0.3	0.2
1061.5	${}^{P}P_{3}(13)$	1062.3	0.8	1.0
	${}^{P}P_{5}(14)$	1061.2	−0.3	0.4
	${}^{P}P_{7}(15)$	1060.3	−1.2	0.2
	${}^{P}P_{9}(16)$	1058.6	−2.9	0.2
	${}^{R}P_{0}(12)$	1060.0	−1.5	1.0
	${}^{R}P_{2}(11)$	1061.3	−0.2	0.5
	${}^{R}P_{4}(10)$	1062.6	1.1	0.3

(To be continued)

Table 10 (continued).

Obs. cm^{-1}	Assignment	Calc. cm^{-1}	Δ (Calc.-obs.)	Calc. relative intensity
1064.5	${}^{P}P_1(12)$	1063.4	−1.1	0.6
	${}^{P}P_6(14)$	1064.8	0.3	0.8
	${}^{R}P_1(11)$	1064.6	0.1	0.6
1067.6	${}^{P}P_2(12)$	1066.5	−1.1	0.7
	${}^{P}P_4(13)$	1065.8	−1.8	0.6
	${}^{P}P_8(15)$	1063.9	−3.7	0.2
	${}^{R}P_0(11)$	1068.0	0.4	1.5
1070.2[a]	${}^{P}P_3(12)$	1070.3	0.1	1.6
	${}^{P}P_5(13)$	1069.3	−0.9	0.6
	${}^{P}P_7(14)$	1068.3	−1.9	0.4
	${}^{P}P_9(15)$	1067.6	−2.6	0.4
	${}^{R}P_2(10)$	1069.3	−0.9	0.6
	${}^{R}P_4(9)$	1070.5	0.3	0.3
1071.0[a]	${}^{P}P_1(11)$	1071.4	0.4	0.9
1073.1	${}^{P}P_4(12)$	1073.9	0.8	0.9
	${}^{P}P_6(13)$	1072.9	−0.2	1.2
	${}^{P}P_8(14)$	1071.9	−1.2	0.4
	${}^{R}P_1(10)$	1072.6	−0.5	0.8
	${}^{R}P_3(9)$	1073.8	0.7	1.0
1076.3	${}^{P}P_2(11)$	1074.9	−1.4	1.0
	${}^{P}P_5(12)$	1076.9	0.6	0.9
	${}^{R}P_0(10)$	1076.0	−0.3	2.0
	${}^{R}P_2(9)$	1077.2	0.9	0.8
1078.5	${}^{P}P_3(11)$	1078.3	−0.2	2.4
	${}^{P}P_7(13)$	1076.4	−2.1	0.6
	${}^{P}P_9(14)$	1075.6	−2.9	0.8
	${}^{R}P_4(8)$	1078.5	0.0	0.3
1079.9	${}^{P}P_1(10)$	1079.4	−0.5	1.2
	${}^{R}P_1(9)$	1080.5	0.6	1.0
1081.9	${}^{P}P_2(10)$	1082.9	1.0	1.5
	${}^{P}P_4(11)$	1081.8	−0.1	1.3
	${}^{P}P_6(12)$	1081.2	−0.7	2.0
	${}^{P}P_8(13)$	1080.0	−1.9	0.6
	${}^{R}P_3(8)$	1081.8	−0.1	1.1
1084.6	${}^{P}P_5(11)$	1085.3	0.7	1.4
	${}^{R}P_0(9)$	1083.9	−0.7	2.7
	${}^{R}P_2(8)$	1085.2	0.6	0.9
1087.1	${}^{P}P_1(9)$	1087.3	0.2	1.7
	${}^{P}P_3(10)$	1086.3	−0.8	3.4

(To be continued)

Table 10 (continued).

Obs. cm^{-1}	Assignment	Calc. cm^{-1}	Δ (Calc.-obs.)	Calc. relative intensity
1087.1	$^{P}P_{7}(12)$	1084.4	−2.7	1.0
	$^{P}P_{9}(13)$	1083.7	−3.4	1.3
1089.3	$^{P}P_{4}(10)$	1089.8	0.5	1.9
	$^{P}P_{6}(11)$	1088.9	−0.4	3.0
	$^{P}P_{8}(12)$	1088.0	−1.3	1.0
	$^{R}P_{1}(8)$	1088.5	−0.8	1.2
	$^{R}P_{3}(7)$	1089.7	0.4	1.0
1091.2	$^{P}P_{2}(9)$	1090.8	−0.4	2.0
	$^{R}P_{0}(8)$	1091.9	0.7	0.9
1092.8	$^{P}P_{5}(10)$	1093.3	0.5	2.1
	$^{P}P_{7}(11)$	1092.4	−0.4	1.5
	$^{P}P_{9}(12)$	1091.7	−1.1	2.0
	$^{R}P_{2}(7)$	1093.1	0.3	0.9
1095.8	$^{P}P_{1}(8)$	1095.3	−0.5	2.1
	$^{P}P_{3}(9)$	1094.2	−1.6	4.6
	$^{P}P_{6}(10)$	1096.9	1.1	4.4
	$^{R}P_{1}(7)$	1096.4	0.6	1.3
1098.0	$^{P}P_{2}(8)$	1098.8	0.8	2.6
	$^{P}P_{4}(9)$	1097.7	−0.3	2.6
	$^{P}P_{8}(11)$	1096.0	−2.0	1.6
1100.5[a]	$^{P}P_{5}(9)$	1101.2	0.7	2.9
	$^{P}P_{7}(10)$	1100.4	−0.1	2.3
	$^{P}P_{9}(11)$	1099.7	−0.8	3.1
	$^{R}P_{0}(7)$	1099.8	−0.7	3.8
1101.5[a]	$^{P}P_{3}(8)$	1102.2	0.7	6.1
1104.6	$^{P}P_{1}(7)$	1103.2	−1.4	2.5
	$^{P}P_{6}(9)$	1104.8	0.2	6.2
	$^{P}P_{8}(10)$	1104.0	−0.6	2.3
1106.3[a]	$^{P}P_{2}(7)$	1106.7	0.4	3.2
	$^{P}P_{4}(8)$	1105.7	−0.6	3.5
1109.1	$^{P}P_{3}(7)$	1110.1	1.0	7.7
	$^{P}P_{5}(8)$	1109.2	0.1	3.9
	$^{P}P_{7}(9)$	1108.3	−0.8	3.3
	$^{P}P_{9}(10)$	1107.7	−1.4	4.7
1113.2	$^{P}P_{4}(7)$	1113.6	0.4	4.5
	$^{P}P_{6}(8)$	1112.8	−0.4	8.5
	$^{P}P_{8}(9)$	1111.9	−1.3	3.4
1114.8	$^{P}P_{2}(6)$	1114.6	−0.2	3.8
	$^{P}P_{9}(9)$	1115.6	0.8	6.8
	$^{R}P_{0}(5)$	1115.6	0.8	4.2

(To be continued)

Table 10 (continued).

Obs. cm^{-1}	Assignment	Calc. cm^{-1}	Δ (Calc.-obs.)	Calc. relative intensity
	${}^PP_3\,(6)$	1118.0	0.4	9.4
1117.6	${}^PP_5\,(7)$	1117.1	−0.5	5.1
	${}^PP_7\,(8)$	1116.3	−1.3	4.5
1119.1[a]	${}^PP_1\,(5)$	1119.0	−0.1	3.1
	${}^PP_2\,(5)$	1122.5	0.7	4.3
	${}^PP_4\,(6)$	1121.5	−0.3	5.6
1121.8	${}^PP_6\,(7)$	1120.7	−1.1	11.4
	${}^PP_8\,(8)$	1119.9	−1.9	4.7
	${}^RQ_{10}$	1122.0	0.2	
1122.8[a]	${}^RP_0\,(4)$	1123.5	0.7	3.8
1123.4[a]	${}^PP_7\,(7)$	1124.2	0.8	6.1
	${}^PP_3\,(5)$	1125.9	−0.2	11.1
1126.1	${}^PP_5\,(6)$	1125.0	−1.1	6.5
	${}^RQ_9$	1125.2	−0.9	3.3
1127.0[a]	${}^PP_1\,(4)$	1126.9	−0.1	3.1
	${}^RQ_8$	1128.3	1.3	
	${}^PP_2\,(4)$	1130.3	0.3	4.6
1130.1	${}^PP_4\,(5)$	1129.4	−0.7	6.8
	${}^PP_6\,(6)$	1128.6	−1.5	14.6
	${}^RQ_7$	1131.5	0.0	
1131.5[a]	${}^PP_5\,(5)$	1132.9	1.4	8.1
	${}^RP_0\,(3)$	1131.3	−0.2	3.0
	${}^RQ_6$	1134.8	0.3	
1134.5	${}^PP_1\,(3)$	1134.7	0.2	2.9
	${}^PP_3\,(4)$	1133.8	−0.7	12.6
	${}^RQ_5$	1138.0	−0.5	
1138.5	${}^PP_2\,(3)$	1138.2	−0.3	4.8
	${}^PP_4\,(4)$	1137.3	−1.2	8.1
	${}^RQ_4$	1141.3	−1.5	
1142.8	${}^PP_1\,(2)$	1142.6	−0.2	2.5
	${}^PP_3\,(3)$	1141.6	−1.2	14.0
1144.4	${}^RQ_3$	1144.6	0.2	
1147.0[a]	${}^PP_2\,(2)$	1146.1	−0.9	4.9
1148.0[a]	${}^RQ_2$	1148.0	0.0	
1151.3	${}^RQ_1$	1151.3	0.0	
	${}^PP_1\,(1)$	1150.3	−1.0	1.8
1154.8	${}^RQ_0$	1154.7	−0.1	100
1158.0	${}^PQ_1$	1158.1	0.1	
1161.3	${}^PQ_2$	1161.6	0.3	
	${}^RR_0\,(0)$	1162.4	1.1	3.8

(To be continued)

Table 10 (continued).

Obs. cm^{-1}	Assignment	Calc. cm^{-1}	Δ (Calc.-obs.)	Calc. relative intensity
1164.9	$^{P}Q_3$	1165.0	0.1	
1167.7	$^{P}Q_4$	1168.5	0.8	
	$^{R}R_1$ (1)	1166.7	−1.0	5.5
	$^{P}Q_5$	1172.0	0.6	
1171.4	$^{R}R_2$ (2)	1171.1	−0.3	8.3
	$^{R}R_0$ (1)	1170.1	−1.3	5.5
1174.7[a]	$^{R}R_1$ (2)	1174.4	−0.3	5.7
1175.2[a]	$^{R}R_3$ (3)	1175.3	0.1	20.2
1175.7	$^{P}Q_6$	1175.6	−0.1	
1177.8	$^{R}R_0$ (2)	1177.8	0.0	6.9
	$^{R}R_2$ (3)	1178.7	0.9	7.9
1179.0[a]	$^{P}Q_7$	1179.1	0.1	
1180.7[a]	$^{R}R_4$ (4)	1179.6	−1.1	10.7
	$^{R}R_1$ (3)	1182.0	−0.8	5.7
1182.8	$^{R}R_3$ (4)	1182.9	0.1	18.1
	$^{P}Q_8$	1182.7	−0.1	
	$^{R}R_0$ (3)	1185.4	0.4	7.7
1185.0	$^{R}R_2$ (4)	1186.3	1.3	7.3
	$^{R}R_5$ (5)	1183.9	−1.1	10.3
1186.1[a]	$^{P}Q_9$	1186.4	0.3	
1187.6	$^{R}R_4$ (5)	1187.2	−0.4	9.1
	$^{R}R_1$ (4)	1189.6	0.2	5.6
1189.4	$^{R}R_3$ (5)	1190.5	1.1	15.7
	$^{R}R_6$ (6)	1188.2	−1.2	18.2
	$^{P}Q_{10}$	1190.0	0.6	
	$^{R}R_5$ (6)	1191.3	−0.9	8.4
1192.2	$^{R}R_7$ (7)	1192.4	0.2	7.5
	P (13) (ν_{3a})	1191.7	−0.5	
	$^{R}R_0$ (4)	1193.0	−0.7	8.0
1193.7	$^{R}R_2$ (5)	1193.9	0.2	6.5
	$^{R}R_4$ (6)	1194.6	0.9	7.6
	$^{R}R_1$ (5)	1197.2	0.6	5.2
1196.6	$^{R}R_6$ (7)	1195.7	−0.9	14.3
	$^{R}R_8$ (8)	1196.6	0.0	5.7
1198.6	$^{R}R_3$ (6)	1197.9	−0.7	13.2
	$^{R}R_5$ (7)	1198.9	0.3	6.7
	$^{R}R_0$ (5)	1200.6	−0.7	7.8
	$^{R}R_2$ (6)	1201.5	0.2	5.6
1201.3[a]	$^{R}R_4$ (7)	1202.2	0.9	6.1
	$^{R}R_7$ (8)	1199.8	−1.5	5.6
	P (12) (ν_{3a})	1201.6	0.3	
1203.5	$^{R}R_6$ (8)	1203.1	−0.4	10.8

(To be continued)

Table 10 (continued).

Obs. cm^{-1}	Assignment	Calc. cm^{-1}	Δ (Calc.-obs.)	Calc. relative intensity
	${}^{R}R_1$ (6)	1204.7	−0.3	4.6
1205.0	${}^{R}R_3$ (7)	1205.5	0.5	10.8
	${}^{R}R_8$ (9)	1204.0	−1.0	4.1
	${}^{R}R_0$ (6)	1208.1	0.4	7.2
1207.7	${}^{R}R_2$ (7)	1208.9	1.2	4.7
	${}^{R}R_5$ (8)	1206.3	−1.4	5.1
	${}^{R}R_7$ (9)	1207.2	−0.5	4.1
	${}^{R}R_1$ (7)	1212.2	0.8	3.9
	${}^{R}R_3$ (8)	1212.9	1.5	8.5
	${}^{R}R_4$ (8)	1209.6	−1.8	4.7
1211.4	${}^{R}R_6$ (9)	1210.5	−0.9	8.0
	${}^{R}R_8$ (10)	1211.4	0.0	2.9
	${}^{R}R_9$ (10)	1208.3	−3.1	5.7
	P (11) (ν_{3a})	1211.3	−0.1	
	${}^{R}R_0$ (7)	1215.6	1.1	6.3
1214.5	${}^{R}R_5$ (9)	1213.7	−0.8	3.8
	${}^{R}R_7$ (10)	1214.6	0.1	2.9
	${}^{R}R_2$ (8)	1216.3	−1.4	3.7
1217.7	${}^{R}R_4$ (9)	1217.0	−0.7	3.5
	${}^{R}R_6$ (10)	1217.9	0.2	5.6
	${}^{R}R_9$ (11)	1215.6	−2.1	3.9
	${}^{R}R_1$ (8)	1219.6	−1.2	3.2
	${}^{R}R_3$ (9)	1220.3	−0.5	6.4
1220.8	${}^{R}R_5$ (10)	1221.1	0.3	2.7
	${}^{R}R_8$ (11)	1218.7	−2.1	2.0
	P (10) (ν_{3a})	1220.8	0.0	
	${}^{R}R_0$ (8)	1223.1	−1.0	5.2
	${}^{R}R_2$ (9)	1223.7	−0.4	2.8
1224.1	${}^{R}R_4$ (10)	1224.4	0.3	2.5
	${}^{R}R_6$ (11)	1225.2	1.1	3.9
	${}^{R}R_7$ (11)	1221.9	−2.2	2.0
	${}^{R}R_9$ (12)	1222.9	−1.2	2.5
	${}^{R}R_1$ (9)	1227.0	−1.0	2.5
1228.0[a]	${}^{R}R_3$ (10)	1227.7	−0.3	4.7
	${}^{R}R_8$ (12)	1226.0	−2.0	1.3
	P (9) (ν_{3a})	1230.2	0.1	
	${}^{R}R_0$ (9)	1230.4	0.3	4.1
1230.1	${}^{R}R_2$ (10)	1231.1	1.0	2.1
	${}^{R}R_5$ (11)	1228.4	−1.7	1.9
	${}^{R}R_7$ (12)	1229.2	−0.9	1.3
1235.9	${}^{R}R_3$ (11)	1235.0	−0.9	3.3
	${}^{R}R_5$ (12)	1235.7	−0.2	1.2

s_{eff} = 1.3–1.9 cm^{-1}. [a] Not resolved.

3. Results

From the rotational analysis values have been derived for the rotational constants A'' and A_i', the Coriolis coupling factors ζ_i, and the band-centre frequencies ν_0. It can be shown[13] that to a good approximation the following expression is valid:

$$A'' = \frac{1}{3}\sum [A_i'(1-\zeta_i) - B_i'] - \frac{1}{3}\sum [(A_i' - A'') - (B_i' - B'')] + \frac{7}{6}B''.$$

As the magnitude of B'' is known (3.880_0 cm^{-1}), A'' can be calculated. From the known values of $B_i' - B''$, $(A_i' - A'') - (B_i' - B'')$, and A'', A_i' can be evaluated for the three perpendicular bands. The values of A_i', B_i', and $A_i'(1-\zeta_i) - B_i'$ have then been used for the calculation of the ζ values. Finally, the band-centre frequencies were obtained from $\nu_0 + A_i'(1-\zeta_i)^2 - B_i'$. The results are given in Table 11. The value $A'' = 5.25_7 \pm 0.02$ cm^{-1} derived here from the analysis of the three perpendicular bands is close to the one (5.245 cm^{-1}) calculated from B'', assuming $r_{CH} = r_{CD}$ and regular tetrahedral structure, and it also compares well with the value 5.243 cm^{-1} obtained from the Raman study of the $\nu_{3\,bc}$ band.[7]

Table 11. Rotational constants A', Coriolis coupling factors ζ, and band-centre frequencies ν_0 for perpendicular bands.

	$\nu_{2\,ab}$	$\nu_{3\,bc}$	$\nu_{4\,bc}$
A_i'(cm^{-1})..................	5.20_2	5.23_5	5.25_5
ζ_i........................	-0.302	0.081	0.588
ν_0(cm^{-1})..................	1471.2	3016.2	1157.7

In Table 12 the results for the $\nu_{3\,bc}$ band are compared with the values obtained from the Raman investigation by Richardson *et al.* (E.H.R.) and the infrared study by Jones (L.H.J.). It is seen that the author's results are in somewhat better agreement with the Raman investigation than with the infrared study.

In Table 13, experimental ζ values are compared with theoretical values calculated recently from force constants by Jones and McDowell,[14] and by Mills.[15] The agreement between the values obtained by the present investigations and the theoretical work seems satisfactory, except in the case of $\zeta_{3\,bc}$.

The sum of the zetas must satisfy the ζ sum rule:[16] $\Sigma\zeta_i = B_e/2A_e$, as far as anharmonicity can be neglected, and no resonances occur. As the "equilibrium" rotational constants, A_e and B_e, are not known, one has to use the

Table 12. Band constant values for the $\nu_{3\,bc}$ band in cm^{-1}.

	Raman[7] E.H.R. et al.	Infrared[14] L.H.J.	This invest.
$A'(1-\zeta)-B'$	0.955	0.924	0.944
$A''-A'\zeta-B''$	0.961	0.920	0.954
$(A'-A'')-(B'-B'')$	−0.0058	0.004	−0.011
$\nu_0+A'(1-\zeta)^2-B'$	3017.17	3017.4	3016.8
A'	5.223	5.24	5.23_5
B'	3.863	3.865	3.87_3
B''	3.877	—	3.88_2
$B'-B''$	−0.0138	−0.013	−0.011
ζ	0.0775	0.08_6	0.081
ν_0	3016.59	3016.9	3016.2
D'_J	5×10^{-5}	5.5×10^{-5} [a]	$5._5\times10^{-5}$
D''_J	4.7×10^{-5}		

[a] Assumed value.

Table 13. Experimental and theoretical ζ values for doubly degenerate normal vibrations.

	$\zeta_{2\,ab}$	$\zeta_{3\,bc}$	$\zeta_{4\,bc}$
Experimental values:			
N. Ginsburg and E. F. Barker	−0.218 to −0.312	0.261 to 0.213	0.625 to 0.692
L. H. Jones		0.08_6	
E. H. Richardson et al.		0.0775	
This investigation	−0.302	0.081	0.588
Theoretical values:			
L. H. Jones and R. S. McDowell	−0.260	0.040	0.589
I. M. Mills	−0.263	0.044	0.588

values for the vibrational ground state. This must, however, be considered a rather good approximation. Thus, the ζ sum rule may be written: $\Sigma\zeta_i = B''/2A'' = 0.370$. The sum of the zetas is 0.367, which should be compared with 0.668 to 0.593 found earlier by Ginsburg and Barker.[17]

A comparison between the present fundamental frequencies and values from previous investigations is given in Table 14. The values adopted here mean a revision of the results of Wilmshurst and Bernstein regarding the fundamentals $\nu_{3\,a}$, $\nu_{4\,a}$, $\nu_{3\,bc}$, and $\nu_{4\,bc}$.

Table 14. Comparison of the present results with previous grating or prism data (cm^{-1}).

Symmetry	Normal vibration	Present investigation	Other investigations	Adopted values
A_1	ν_1	2948*	2945[a]	2948
	ν_{3a}	2210*	2200[a]	2210
			2200.03[b]	
	ν_{4a}	1306.5	1306.8[c]	1306.5
			1300[a]	
E	ν_{2ab}	1471.2	1477.1[c]	1471.2
			1471[a]	
	ν_{3bc}	3016.2	3021[a]	3016.6
			3016.9[d]	
			3016.59[e]	
	ν_{4bc}	1157.7	1156.3[c]	1157.7
			1155[a]	

[a] See Ref. 5.
[b] See Ref. 3.
[c] See Ref. 17.
[d] See Ref. 6.
[e] See Ref. 7.

* Estimated unperturbed frequency (see page 6).

IV. Overtones and Combinations

Overtone and combination bands have been observed in the region 2000–6000 cm^{-1}. Thirty-six pronounced absorption bands have been measured and interpreted as summation bands. It was possible to explain sixteen bands as binary combinations, whereas the rest of the bands have been interpreted as ternary and quaternary summation bands. Only in three cases, however, it has been necessary to make use of quaternary combinations.

The results are given in Table 15. In the column with observed frequencies square brackets indicate the possible presence of Fermi resonance, which makes definite assignments uncertain.

Only below 5000 cm^{-1} the bands have been characterized as parallel ($\parallel$) or perpendicular ($\perp$) bands. The reason for this is the limited resolving power of the spectrograph at high frequencies and the increased possibility of interactions between bands, which may change the shape of the bands considerably.

For the calculation of the combination frequencies, observed frequencies have been used rather than calculated values. In some cases this gives more

Table 15. Possible assignments of overtones and combinations.

Assignment	Symmetry	Band structure obs.	Intensity	Frequency (cm^{-1}) Obs.	Frequency (cm^{-1}) Calc.	Δ (Calc.-obs.)
$4bc+4bc$	A_1+E	$\parallel$	s	2316[a]	2315	-1
$4a+4bc$	E		vw	ca. 2460	2464	ca. $+4$
$4a+4a$	A_1	$\parallel$	w	2597	2613	$+16$
$2ab+2ab$	A_1+E		s	2910[a]	2942	$+32$
$3a+4bc$	E	$\parallel$	w	3337	3358	$+21$
$3a+4a$	A_1		m	3498	3506	$+8$
$4a+4bc+4bc$	A_1+E		vw	3617	3622	$+5$
$2ab+3a$	E		vw	3670	3671	$+1$
$4a+4a+4bc$	E	$\perp$	vw	ca. 3750	3771	ca. $+21$
$2ab+4bc+4bc$	A_1+A_2+2E	$\perp$	vw	ca. 3795	3787	ca. -8
$4a+4a+4a$	A_1		vw	3874	3919	$+45$
$2ab+4a+4a$	E		w	4056	4084	$+28$
$2ab+2ab+4bc$	A_1+A_2+2E		w	4072	4100	$+28$
$1+4bc$	E	$\perp$	w	ca. 4126	4128	$+2$
$2ab+2ab+4a$	A_1+E	$\parallel$	vw	4216[b]	4249	$+33$
$3bc+4a$	E	$\perp$	w	4313	4323	$+10$
$3a+3a$	A_1	$\parallel$	vw	4342	4400	$+58$
$2ab+3bc$	A_1+A_2+E		w	4474	4488	$+14$
$3a+4a+4a$	A_1		vvw	4783	4813	$+30$
$4a+4a+4bc+4bc$	A_1+E		vvw	4902	4928	$+26$
$2ab+4bc+4bc+4bc$	A_1+A_2+3E				4944	$+42$
$2ab+3a+4a$	E	$\perp$	vvw	4962	4978	$+16$
$2ab+2ab+3a$	A_1+E		vw	5105	5142	—
$1+3a$	A_1	$\parallel$	vw	5164	5170	—
$3a+3bc$	E		vw	5223	5217	—
$1+4bc+4bc$	A_1+E		vw	5257	5285	—
$3bc+4bc+4bc$	A_1+A_2+2E		vw	5311	5332	—
$2ab+4a+4a+4a$	E		vw	5367	5391	$+26$
$3a+3a+4bc$	E		vvw	5494	5558	—
$2ab+2ab+4a+4a$	A_1+E		vvw	5558	5555	—
$2ab+2ab+2ab+4bc$	A_1+A_2+3E				5571	—
$1+4a+4a$	A_1		vw	5585	5583	—
$1+2ab+4bc$	A_1+A_2+E				5599	—
$3bc+4a+4a$	E		vw	5626	5630	—
$3a+3a+4a$	A_1		vvw	5692	5706	$+14$
$1+1$	A_1		w	5762	5940	—
$2ab+3a+3a$	E		w	5860	5871	—
$1+3bc$	E		w	5983	5987	—
$3bc+3bc$	A_1+E		w	6024	6033	—

[a] Displaced by Fermi resonance with fundamental.

[b] CH_4?

reasonable agreement between calculated and observed frequencies. Also from a theoretical point of view this procedure is the more correct.

In general quite large negative anharmonicities are observed, e.g. the difference $\nu_{\text{calc.}} - \nu_{\text{obs.}}$ is positive. However, a few of the observed combination frequencies show small positive anharmonicities.

The prominent absorption at 6024 cm^{-1} has been interpreted as the first overtone of the carbon-hydrogen stretching frequency, $3\,bc + 3\,bc$, the anharmonicity being -7 cm^{-1}. This anharmonicity is, however, much smaller than one should expect for the first overtone of a C–H stretching frequency, in which case an anharmonicity of the magnitude of -100 to -200 cm^{-1} would seem reasonable. A probable explanation is that the band, because of Fermi resonance, has been displaced towards higher wave-numbers. Another possibility would be that the band is the quaternary combination $3\,a + 4\,a + 4\,a + 4\,a$, the calculated frequency being 6120 cm^{-1}. The observed intensity of the band, however, seems too high for a quaternary combination, although Fermi resonance may have increased it.

Generally, it must be emphasized that on account of the great anharmonicities and the possible effects of Fermi resonance and other interactions, the assignment of the bands to specific combinations, especially in the region 5000–6000 cm^{-1}, is only tentative.

Acknowledgments

I am greatly indebted to the late Professor A. Langseth for suggesting the present investigation, for many helpful discussions on the subject and for much good advice. My thanks are also due to Dr. Svend Brodersen for having recorded the spectra on the infrared spectrometer.

Note added in proof: A calculation of the unperturbed frequencies using first-order perturbation theory[18] and assuming that the intensity ratio $I\,(2\,\nu_{2\,ab})/I\,(\nu_1) = 0.5$ (see Fig. 1) gives $2\,\nu_{2\,ab} = 2930$ cm^{-1} and $\nu_1 = 2950$ cm^{-1}.

References

1. See G. Herzberg, Infrared and Raman Spectra of Polyatomic Molecules (D. van Nostrand Co., New York, 1945), p. 306 and 309.
2. D.R.J. Boyd and H.W. Thompson, Proc. Roy. Soc. **A216**, 143 (1953).
3. Harry C. Allen, Jr., and Earle K. Plyler, J. of Research of the Nat. Bur. of Standards **63A**, 145 (1959).
4. D. G. Rea and H. W. Thompson, Trans. Faraday Soc. **52**, 1304 (1956).
5. J. K. Wilmshurst and H. J. Bernstein, Canad. Journ. Chem. **35**, 226 (1957).
6. Llewellyn H. Jones, J. Mol. Spectroscopy **4**, 84 (1960).
7. E. H. Richardson, S. Brodersen, L. Krause, and H. L. Welsh, to be published (private communication from Dr. Brodersen).
8. Svend Brodersen and A. Langseth, Mat. Fys. Skr. Dan. Vid. Selsk. **1**, no. 1 (1956).
9. Svend Brodersen, J. Opt. Soc. Am. **43**, 877 (1953).
10. Janet Hawkins Meal and S.R. Polo, J. Chem. Phys. **24**, 1126 (1956).
11. G. Herzberg, *loc. cit.* p. 436.
12. G. Herzberg, *loc. cit.* p. 426.
13. F. Allan Andersen, Børge Bak, and Svend Brodersen, J. Chem. Phys. **24**, 989 (1956).
14. Llewellyn H. Jones and Robin S. McDowell, J. Mol. Spectroscopy **3**, 632 (1959).
15. I.M. Mills, Spectrochim. Acta **16**, 35 (1960).
16. W. H. Schaffer, J. Chem. Phys. **10**, 1 (1942).
17. Nathan Ginsburg and E.F. Barker, J. Chem. Phys. **3**, 668 (1935).
18. G. Herzberg, *loc. cit.* p. 216.

Indleveret til Selskabet den 31. marts 1962.
Færdig fra trykkeriet den 20. maj 1963.